World Journal of

Gastroenterology

Contents

ABOUT COVER

Editorial Board Member of *World Journal of Gastroenterology*, Vishal Sharma, MD, DM, Associate Professor, Department of Gastroenterology, Postgraduate Institute of Medical Education and Research, Chandigarh 160012, India. sharma.vishal@pgimer.edu.in

AIMS AND SCOPE

The primary aim of *World Journal of Gastroenterology* (*WJG*, *World J Gastroenterol*) is to provide scholars and readers from various fields of gastroenterology and hepatology with a platform to publish high-quality basic and clinical research articles and communicate their research findings online. *WJG* mainly publishes articles reporting research results and findings obtained in the field of gastroenterology and hepatology and covering a wide range of topics including gastroenterology, hepatology, gastrointestinal endoscopy, gastrointestinal surgery, gastrointestinal oncology, and pediatric gastroenterology.

INDEXING/ABSTRACTING

The *WJG* is now indexed in Current Contents®/Clinical Medicine, Science Citation Index Expanded (also known as SciSearch®), Journal Citation Reports®, Index Medicus, MEDLINE, PubMed, PubMed Central, and Scopus. The 2021 edition of Journal Citation Report® cites the 2020 impact factor (IF) for *WJG* as 5.742; Journal Citation Indicator: 0.79; IF without journal self cites: 5.590; 5-year IF: 5.044; Ranking: 28 among 92 journals in gastroenterology and hepatology; and Quartile category: Q2. The *WJG*'s CiteScore for 2020 is 6.9 and Scopus CiteScore rank 2020: Gastroenterology is 19/136.

RESPONSIBLE EDITORS FOR THIS ISSUE

ORIGINAL ARTICLE

Basic Study

Fusobacterium nucleatum promotes colon cancer progression by changing the mucosal microbiota and colon transcriptome in a mouse model

Na Wu, Yu-Qing Feng, Na Lyu, Di Wang, Wei-Dong Yu, Yong-Fei Hu

Na Wu, **Di Wang**, **Wei-Dong Yu**, Department of Central Laboratory & Institute of Clinical Molecular Biology, Peking University People's Hospital, Beijing 100044, China

Yu-Qing Feng, **Yong-Fei Hu**, State Key Laboratory of Animal Nutrition, College of Animal Science and Technology, China Agricultural University, Beijing 100193, China

Na Lyu, CAS Key Laboratory of Pathogenic Microbiology and Immunology, Institute of Microbiology, Chinese Academy of Sciences, Beijing 100101, China

Corresponding author: Yong-Fei Hu, PhD, Professor, State Key Laboratory of Animal Nutrition, College of Animal Science and Technology, China Agricultural University, No. 2 Yuanmingyuan West Road, Haidian District, Beijing 100193, China. huyongfei@cau.edu.cn

Abstract

BACKGROUND
Fusobacterium nucleatum (*F. nucleatum*) has long been known to cause opportunistic infections and has recently been implicated in colorectal cancer (CRC), which has attracted broad attention. However, the mechanism by which it is involved in CRC development is not fully understood.

AIM
To explore its potential causative role in CRC development, we evaluated the colon pathology, mucosa barrier, colon microbiota and host transcriptome profile after *F. nucleatum* infection in an azoxymethane/dextran sulfate sodium salt (AOM/DSS) mouse model.

METHODS
Three groups of mice were compared to reveal the differences, *i.e.*, the control, AOM/DSS-induced CRC and AOM/DSS-FUSO infection groups.

RESULTS
Both the AOM/DSS and AOM/DSS-FUSO groups exhibited a significantly reduced body weight and increased tumor numbers than the control group, and AOM/DSS mice with *F. nucleatum* infection showed the highest tumor formation ratio among the three groups. Moreover, the colon pathology was the most serious in the AOM/DSS-FUSO group. We found that the structure of the colon

microbiota changed considerably after *F. nucleatum* infection; striking differences in mucosal microbial population patterns were observed between the AOM/DSS-FUSO and AOM/DSS groups, and inflammation-inducing bacteria were enriched in the mucosal microbiota in the AOM/DSS-FUSO group. By comparing intestinal transcriptomics data from AOM *vs* AOM/DSS-FUSO mice, we showed that transcriptional activity was strongly affected by dysbiosis of the gut microbiota. The most microbiota-sensitive genes were oncogenes in the intestine, and the cyclic adenosine monophosphate signaling pathway, neuroactive ligand–receptor interaction, PPAR signaling pathway, retinol metabolism, mineral absorption and drug metabolism were highly enriched in the AOM/DSS-FUSO group. Additionally, we showed that microbial dysbiosis driven by *F. nucleatum* infection enriched eight taxa belonging to Proteobacteria, which correlates with increased expression of oncogenic genes.

CONCLUSION

Our study demonstrated that *F. nucleatum* infection altered the colon mucosal microbiota by enriching pathogens related to the development of CRC, providing new insights into the role of *F. nucleatum* in the oncogenic microbial environment of the colon.

Key Words: *Fusobacterium nucleatum*; Mucosal microbiota; Transcriptome; Colorectal cancer; Inflammation-inducing bacteria

Core Tip: *Fusobacterium nucleatum* (*F. nucleatum*) has long been known to cause oppo-rtunistic infections and has recently been implicated in colorectal cancer (CRC). However, the mechanism by which it is involved in CRC development is not fully understood. Here, striking differences in mucosal microbial population patterns were observed and inflammation-inducing bacteria were enriched in the mucosal microbiota in the azoxymethane/dextran sulfate sodium salt-FUSO group. We showed that transcriptional activity was strongly affected by dysbiosis of the gut microbiota. Additionally, we showed that microbial dysbiosis driven by *F. nucleatum* infection enriched eight taxa belonging to Proteobacteria, which correlates with increased expression of oncogenic genes.

INTRODUCTION

Colorectal cancer (CRC) is the third most common cancer and the fourth leading cause of cancer death worldwide[1]. The incidence of CRC in China has increased dramatically during the past decade[2].

Fusobacterium nucleatum (*F. nucleatum*), a gram-negative anaerobe, was recently identified as an emerging pathogen that has been frequently found in CRC[3-5]. Importantly, overload of *F. nucleatum* was found to be associated with an advanced tumor stage and a poor prognosis in CRC[6]. Accumulating evidence has revealed that *F. nucleatum* influences different stages of CRC progression. *F. nucleatum* can promote the initiation and development of CRC by adhering to epithelial cells through its unique FadA protein[7], which can bind vascular endothelial cadherin and alters endothelial integrity [8]. The activation of oncogenic miR21 under *F. nucleatum* stimulation results in the overexpression of TLR-4/nuclear factor-kappaB, increasing the proliferation of CRC cells and promoting tumor development[9]. Once a colon tumor has developed, *F. nucleatum* can adhere to Gal-GalNAc-expressing tumor cells by binding to the Fap2 Lectin, leading to enrichment of *F. nucleatum*[10]. *F. nucleatum* infection was also proven to increase the expression levels of inflammatory genes, transcription factors, and oncogenes[8,11]. These studies enhance our knowledge of the mechanisms by which *F. nucleatum* shapes the tumor microenvironment.

Evidences have revealed that the local microbiota is also an important part of the tumor microenvironment. Gut microbiota dysbiosis can reshape the tumor microenvironment and make it favorable for tumor growth[12]. The mechanisms involved include increasing mutagenesis, regulation of oncogenic pathways, and modulation of host immune system[13]. These oncogenic functions of gut microbiota are probably due to the microbial products or metabolites they produce when the community structure

balance is disrupted and a resulting overgrowth of specific bacteria. For example, the overload of colibactin-producing *Escherichia coli* and other Enterobacteriaceae can induce DNA damage of host cells and exert tumorigenic effect[14]. These facts suggest a close relationship between gut microbiota, the tumor microenvironment, and CRC. However, the regulatory role of *F. nucleatum* in the "oncogenic microbial environment" of the colon remains mostly unknown. Revealing the effects of *F. nucleatum* infection on the changes of mucosal microbiota will help to provide further insight into the mechanisms of the tumorigenic effect of *F. nucleatum*.

In the present study, we explored the role of *F. nucleatum* in the development of CRC and in altering the mucosal microbial community structure and investigated the association between microbial dysbiosis and the expression of oncogenic signaling pathways. *F. nucleatum* strain ATCC 25586 was gavaged into azoxymethane/dextran sulfate sodium salt (AOM/DSS) mice to explore the role of *Fusobacterium* overload in the progression of intestinal adenoma against a background of environmental inflammatory factors. RNA-seq transcriptomic analysis was used to identify the differentially expressed gene (DEG) signatures driven by *F. nucleatum* infection, and integrated network analysis was conducted to reveal the relationship between microbial dysbiosis and the DEGs. Our study lays a foundation for understanding the regulatory role of *F. nucleatum* in the oncogenic microbial environment of the colon.

MATERIALS AND METHODS

Bacterial strain and culture conditions
The *F. nucleatum* strain ATCC 25586 was purchased from American Type Culture Collection (ATCC) and was cultured as described previously[3]. In brief, *F. nucleatum* was grown in Columbia blood agar supplemented with 5 mg/mL haemin, 5% defibrinated sheep blood, and 1 mg/mL Vitamin K1 in an anaerobic condition with 85% N_2, 10% H_2, and 5% CO_2 at 37 °C. And 10^9 colony-forming units *per* mL (CFU/mL) were prepared for *F. nucleatum* colonization.

Animal model
Thirty-six conventional C57BL/6J wild-type male mice (4 wk of age) were obtained from the Beijing Animal Study Centre and maintained in the Laboratory Animal Services Centre at the Chinese Center for Disease Control and Prevention. The Institutional Animal Care Committee of the Peking University People's Hospital approved all animal experimentation.

To create the mouse model of colon neoplasia induced by AOM/DSS-induced colon neoplasia[15], 24 mice at 6 wk of age were injected intraperitoneally with a single dose of 10 mg/kg AOM (Sigma), designated week 0. DSS (MP Biochemicals; 36000-50000 mw) was dissolved in filtered drinking water and administered to the mice for 7 d during the following weeks: Weeks 1 (1% DSS), 3 (1% DSS), and 5 (1% DSS). After 1 wk of AOM/DSS treatment, the 24 mice were divided into 2 groups, each with 12 mice. At week 7 they were orally gavaged daily with 10^9 CFU/mL (in 100 µL volume for each mouse) *F. nucleatum* (AOM/DSS-FUSO group) or phosphate-buffered saline (AOM/DSS group) for two weeks. The 12 mice in the control group were sibling littermates and received no treatment.

After 2 wk after *Fusobacterium* inoculation as previous study described[16], the mice were sacrificed, colon mucosal contents were collected for microbiota profiling, the colons were dissected, and the polyps were counted. For a subset of the samples, the distal portion of the colon was fixed in 4% paraformaldehyde, paraffin-embedded, and sectioned for hematoxylin and eosin staining. The remaining colon tissue was then prepared for RNA sequencing.

The body weight, colon length, colorectal tumor formation ratio, immune cell patterns, gut microbiota structure and intestine transcriptomics were assessed to explore the potential role of ATCC 25586 in the carcinogenesis/development of CRC.

Histological evaluation
The colon segments were submitted for histological processing. All slides were stained with hematoxylin and eosin. Dysplasia was assessed by the presence of hyperchromasia, nuclear pleomorphism, and increased nuclear-to-cytoplasmic ratios.

Immunohistochemical staining
The expression of E-cadherin and Ki-67 was determined by immunohistochemistry staining. Serial 3 mm sections of the formalin-fixed paraffin-embedded colon tissues on the slides were heated in a microwave with sodium citrate for antigen repair, followed by 2% goat serum for blocking. The slides were then treated with mouse anti-E-cadherin (BD Biosciences, catalog 610181) and anti-Ki-67 (Cell Signaling Technology, catalog 9192) overnight at 4 °C, visualized with diaminobenzidine, counter-stained with hematoxylin, dehydrated and mounted. Staining index of Ki-67 immunostaining was determined by percentage of positive cells having brown nuclear staining from three randomly selected fields at 400 × magnification.

Microbial DNA extraction and 16S rRNA gene sequencing

Microbiota DNA from the colon mucosal contents was extracted using the QIAamp DNA Stool Mini Kit (Qiagen, catalog 51604). For all samples, polymerase chain reaction (PCR) amplification of the 16S rRNA gene with the V3-V4 variable regions was performed using the primers 341F (5'-CCTAYGG-GRBGCASCAG-3') and 806R (5'-GGACTACNNGGGTATCTAAT-3')[17]. The pooled library was sequenced on the Ion S5™ XL System (Thermo Fisher Scientific). Single-end reads were assigned to the samples based on their unique barcodes and trimmed by removing the barcodes and primer sequences. Raw fastq files were quality-filtered using fastp[18]. Chimeric sequences were detected and removed by vsearch software[19]. Operational taxonomic units (OTUs) were clustered with 97% identity using UPARSE v7.0.1001[20]. The most frequent sequences were selected as the representative sequences for each OTU. Representative sequences for each OTU were annotated using Mothur software at Threshold: 0.8-1 against the SILVA V132 database (http://www.arb-silva.de/) at each taxonomic rank (kingdom, phylum, class, order, family, genus and species)[21]. OTU abundance information was normalized using a standard sequence number corresponding to the sample with the fewest sequences. To avoid biases, the normalized data were subjected to alpha diversity and beta diversity analyses. Alpha diversity indices (Chao1, ACE, Shannon index, Simpson) and UniFrac distance were calculated by QIIME v1.9.1[22,23]. Beta diversities were visualized by principal coordinate analysis (PCoA) and nonmetric multidimensional (NMDS) based on Bray–Curtis dissimilarity.

Quantitative real-time PCR for F. nucleatum

The Q-PCR assay was performed to determine the colonization of *F. nucleatum.* The 16S primers for *F. nucleatum* quantification were F-TGCGATAAGCCTAGATAAGTTGCA and R-CTTAATAGAT-TGCTCCATTCGGAAA. Primers for total bacterial DNA were F-ACTCCTACGGGAGGCAGCAGT and R-GTATTACCGCGGCTGCTGGCAC[16]. The level of *F. nucleatum* was evaluated by the following formula: The relative value (RV) of *F. nucleatum* was determined by the $2^{-\Delta ct}$ method using total bacterial level as a normalizer. The relative abundance (RA) of *F. nucleatum* was scaled to a reasonable range with the following equation: RA = $\log_2$ (RV × 10000 + 1).

RNA extraction and RNA sequencing

Total RNA was isolated using TRIzol reagent (Invitrogen, Carlsbad, CA) according to the manufacturer's recommendations. A total of 3 μg RNA *per* sample was used as the input material for the RNA sample preparations. Sequencing libraries were generated using the NEBNext® UltraTM RNA Library Prep Kit for Illumina® (NEB, United States) following the manufacturer's recommendations. The library preparations were sequenced on an Illumina platform, and 150 bp paired-end reads were generated.

The raw reads were first processed through in-house Perl scripts. Adaptor sequences, duplicated sequences, poly-N reads containing more than 10% "N", and low-quality reads containing more than 50% bases with Q ≤ 5 were removed to obtain high-quality clean reads. Clean reads were aligned to the reference genome using Hisat2 v2.0.5[24]. FeatureCounts v1.5.0-p3 was used to count the read numbers mapped to each gene[25]. Then, the FPKM of each gene was calculated based on the length of the gene and the read count mapped to this gene. Prior to the differential gene expression analysis, for each sequenced library, the read counts were adjusted by the edgeR package. Differential gene expression analysis of the two conditions was performed using the edgeR package v3.18.1. The *P* values were adjusted using the Benjamini & Hochberg method[26]. A corrected *P* value of 0.05 and absolute fold change of 2 were set as the thresholds for significantly DEGs. Gene Ontology (GO) enrichment analysis of the DEGs was implemented by the clusterProfiler R package. GO terms with corrected *P* values less than 0.05 were considered significantly enriched by the DEGs. We used the clusterProfiler R package to test the statistical enrichment of the DEGs in the KEGG pathways[27].

Statistical analysis and visualization

The Kruskal–Wallis test was performed when comparing samples from more than two groups. The difference in ratio of diarrhea and bloody was assessed using Chi-square measure. Permutational multivariate analysis was applied with a parameter of 999 permutations in R[28]. Linear discriminant analysis effect size (LEfSe) was used to estimate which microbiome attributes differed significantly by treatments[29]. The relationship between the gut microbiota and DEGs was determined by calculating Spearman's correlations, and then network visualization was performed using Cytoscape v3.6.1[30]. Heatmaps were generated using the R package pheatmap (https://github.com/raivokolde/pheatmap). The relationship between the different gut microbiota and the pathways was determined by calculating Spearman's correlations. The R package ggplot2 was used for the other data visualization in the figures in the present study.

Ethics statement

All animal protocols were approved by the Animal Experimentation Ethics Committee of the Peking University People's Hospital in China. The experiments were conducted in accordance with the Animal Research: Reporting of in Vivo Experiments (ARRIVE) guidelines.

RESULTS

F. nucleatum infection promotes the development of CRC

A flow chart illustrating the *F. nucleatum* infection strategy combined with AOM/DSS treatment is shown in Figure 1A. The colonization of *F. nucleatum* was confirmed by 16S-sequencing and Q-PCR (Supplementary Figure 1). The body weight of the mice in each group increased slowly (Figure 1B), and it differed significantly between the control mice and the AOM/DSS models (two-way ANOVA, $P <$ 0.05). After AOM/DSS treatment for six weeks, four mice in the AOM/DSS group and six mice in the AOM/DSS-FUSO group developed diarrhea and bloody stools (Chi-square, $P >$ 0.05). No bloody stool was observed in the control group. Over the eight-week treatment, only three mice in the AOM/DSS group and five mice in the AOM/DSS-FUSO group survived.

The AOM/DSS-FUSO group had a trend but not significantly reduced colon length than the AOM/DSS group (Figure 1C), and AOM/DSS-FUSO had the highest tumor formation ratio among the three groups (Figure 1D). The AOM/DSS mice exhibited histological inflammation. In addition, the colon pathology was the most serious in the AOM/DSS-FUSO group, which was confirmed by hematoxylin-eosin (H&E) staining (Figure 1E). The presence of hyperchromasia and nuclear pleomorphism were observed in the AOM/DSS-FUSO group. We also found increased epithelial cell proliferation in the colons of AOM/DSS-FUSO mice, as indicated by a higher expression of Ki-67 than in the other two groups (Supplementary Figure 2). The abnormal expression of E-cadherin in the AOM/DSS-FUSO mice reflected the impaired function of the intestinal barrier.

Aberrant activation of epithelial-mesenchymal transition (EMT) is considered an important trigger of cancer invasion and metastasis[31]. The AOM/DSS-FUSO colon tissues showed morphological features of partial EMT, which was not observed in the AOM/DSS model (Figure 1E). In addition to the morphology-based analysis of colon tissue by H&E staining, the assessment of E-cadherin expression by immunohistochemistry can support the evaluation of partial EMT[31]. The expression of the barrier protein E-cadherin was modestly reduced in the AOM/DSS-FUSO group. Loss of the prototypical epithelial barrier protein E-cadherin is an additional sign of partial EMT[32]. The abnormal histology changes and the reduction of E-cadherin in AOM/DSS-FUSO mouse colons indicated that the AOM/DSS mice with *F. nucleatum* infection had undergone partial EMT, which is critical for CRC progression.
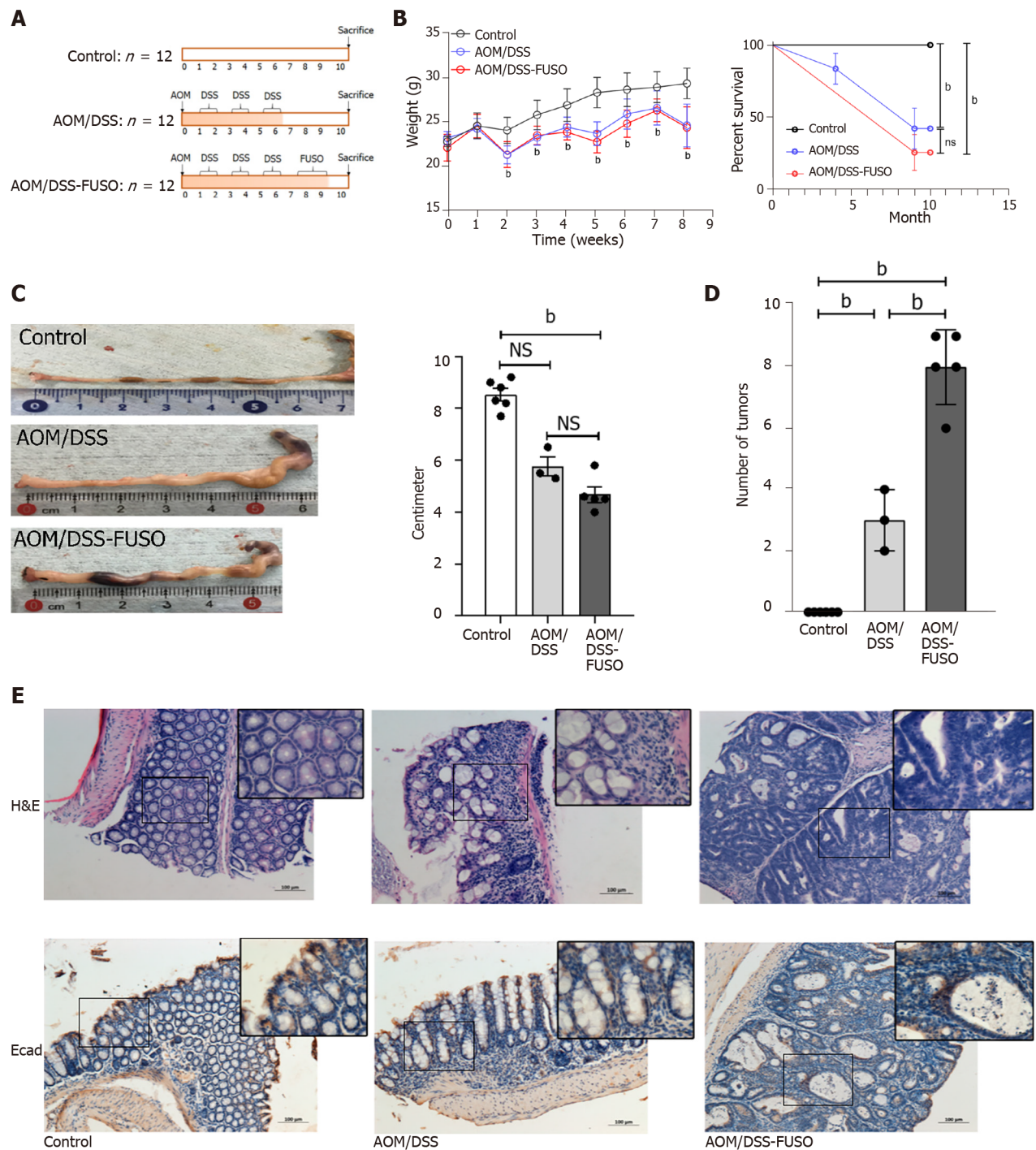
F. nucleatum infection changes the mucosal microbiota community structure

To investigate the effect of *F. nucleatum* infection on the mucosal microbiota, we compared the mucosal microbial composition of the three groups. The β diversity was very different among the three groups. The control group was clearly separated from the AOM/DSS-FUSO and AOM/DSS groups, as shown in the NMDS analysis (Figure 2A). This trend was also found in the PCoA analysis and was confirmed by the weighted UniFrac distance (Figure 2B and C). Around 12.8% of the bacterial composition variance could be explained by the addition of *F. nucleatum* (Permutation based analysis of variance). In AOM/DSS models, AOM/DSS-FUSO and AOM/DSS mice developed different mucosal microbiota with *F. nucleatum* infection as a significant factor in driving the differences. We then assessed the shared and unique OTUs in the AOM/DSS and AOM/DSS-FUSO groups to detect the effect of *F. nucleatum* infection. We observed that the AOM/DSS-FUSO group had more unique OTUs, approximately 44.9% (1117/2490), than the AOM/DSS group, 24.9% (456/1829), signifying that *F. nucleatum*-infected mice largely harbor unique inhabitant niches (Figure 2D). The Shannon, Simpson, observed species, and Chao1 indices for alpha diversity showed no significant differences among the three groups (Supplementary Figure 3).

Differentially abundant mucosal microbial taxa driven by F. nucleatum infection

We then explored the specific microbial members related to *F. nucleatum infection*. First, we compared the bacterial RA between groups at different taxa levels. We showed that the phylum Proteobacteria and eight other potential pathogens belonging to Proteobacteria (LEfSe, Figure 3A and B) were the dominant taxa in AOM/DSS-FUSO mice. Meanwhile, the phylum Bacteroides and the family Bacteroidaceae were enriched in AOM/DSS mice, which were evident CRC signature taxa[33]. The enrichment of potential pathogenic taxa and depletion of probiotic bacteria such as Lactobacillales were features of the mucosal microbiota caused by *F. nucleatum* infection (Figure 3C). Comparing the two CRC model groups, the mucosal microbiota in the control mice was dominated by the phylum Firmicutes and the probiotic taxa (Figure 3A and B).

We further compared the distribution of the top 50 most abundant taxa among the three groups. We found that the mucosal microbial population patterns were different in the three groups; the structure of the colon mucosal microbiota changed considerably after *F. nucleatum* infection in the AOM/DSS-FUSO mice (Figure 3D). Inflammation-inducing bacteria were significantly enriched in the mucosa microbiota of AOM/DSS-FUSO group compared with AOM/DSS group, such as *Denitratisom*, *Stenotrophomonas* and unidentified Enterobacteriaceae ($P =$ 0.036, 0.018, and 0.048, respectively, wilcon rank-sum test, one-sided), while the potential probiotic genera were remarkably less abundant in AOM/DSS-FUSO group, such as unidentified Ruminococcaceae, unidentified Lachnospiraceae, and *Akkermansia* ($P =$ 0.036, 0.036,
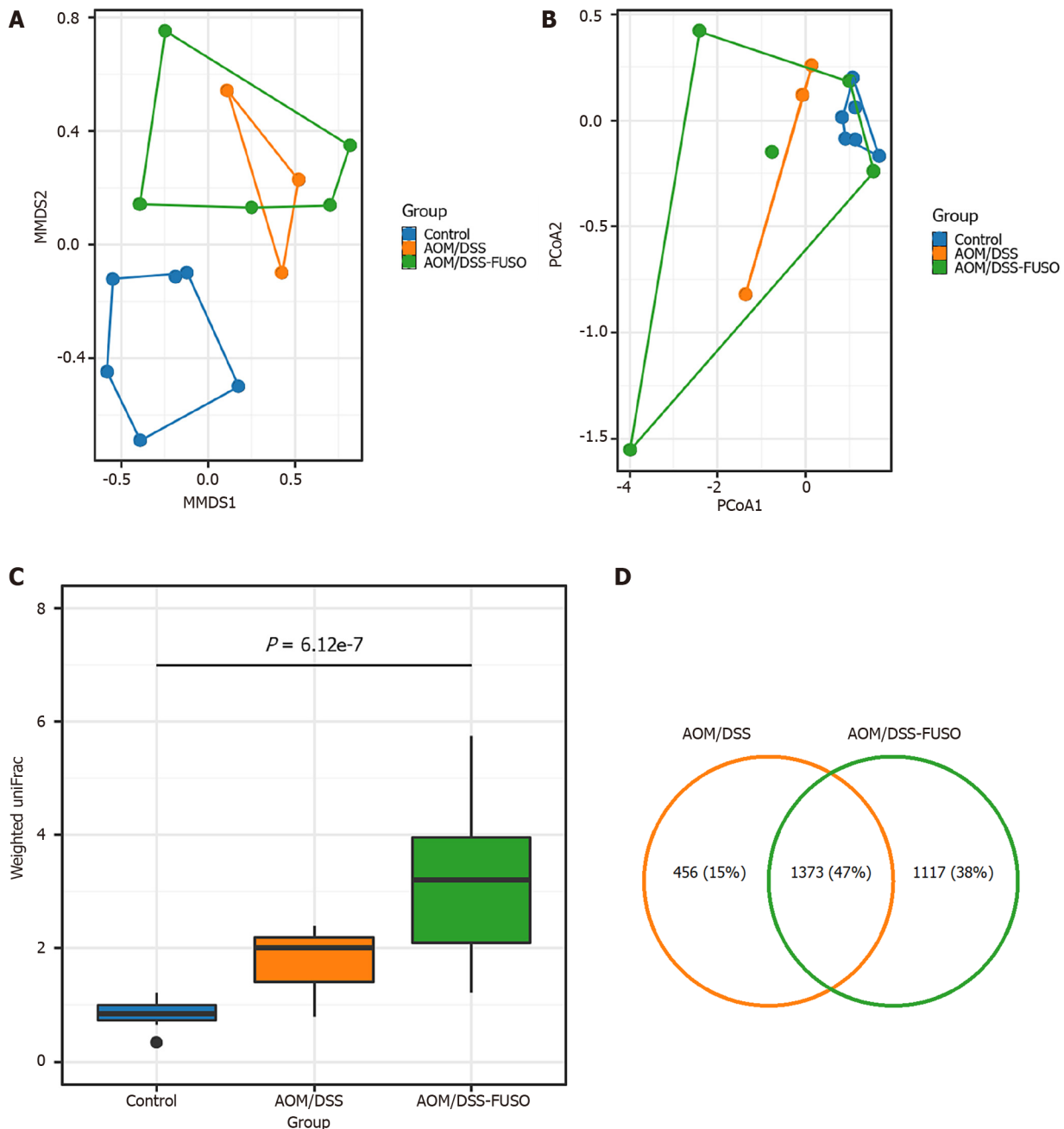
Figure 1 Effect of *F. nucleatum* infection on colon carcinogenesis in the azoxymethane/dextran sulfate sodium-induced model. A: Experimental design illustrating the *F. nucleatum* infection strategy combined with azoxymethane/dextran sulfate sodium salt treatment; B: The body weight and survival curve of the three groups during the experiment was evaluated with two-way ANOVA; C: The colon lengths of the three groups were compared using a t-test; D: The numbers of tumors in the colon of the three groups were compared using a t-test; E: Hematoxylin-eosin staining and immunohistochemistry of E-cadherin-positive cells in the colon of the three groups. $^aP < 0.05$; $^bP < 0.01$. NS: No signification; AOM: Azoxymethane; DSS: Dextran sulfate sodium salt.

and 0.071, respectively, wilcon rank-sum test, one-sided). Taken together, these results suggested that *F. nucleatum* infection further worsens the dysbiosis of the colon mucosal microbiota by increasing the abundance of pathogenic bacteria while reducing probiotics.

Altered host signaling pathways in colon tissue under F. nucleatum infection
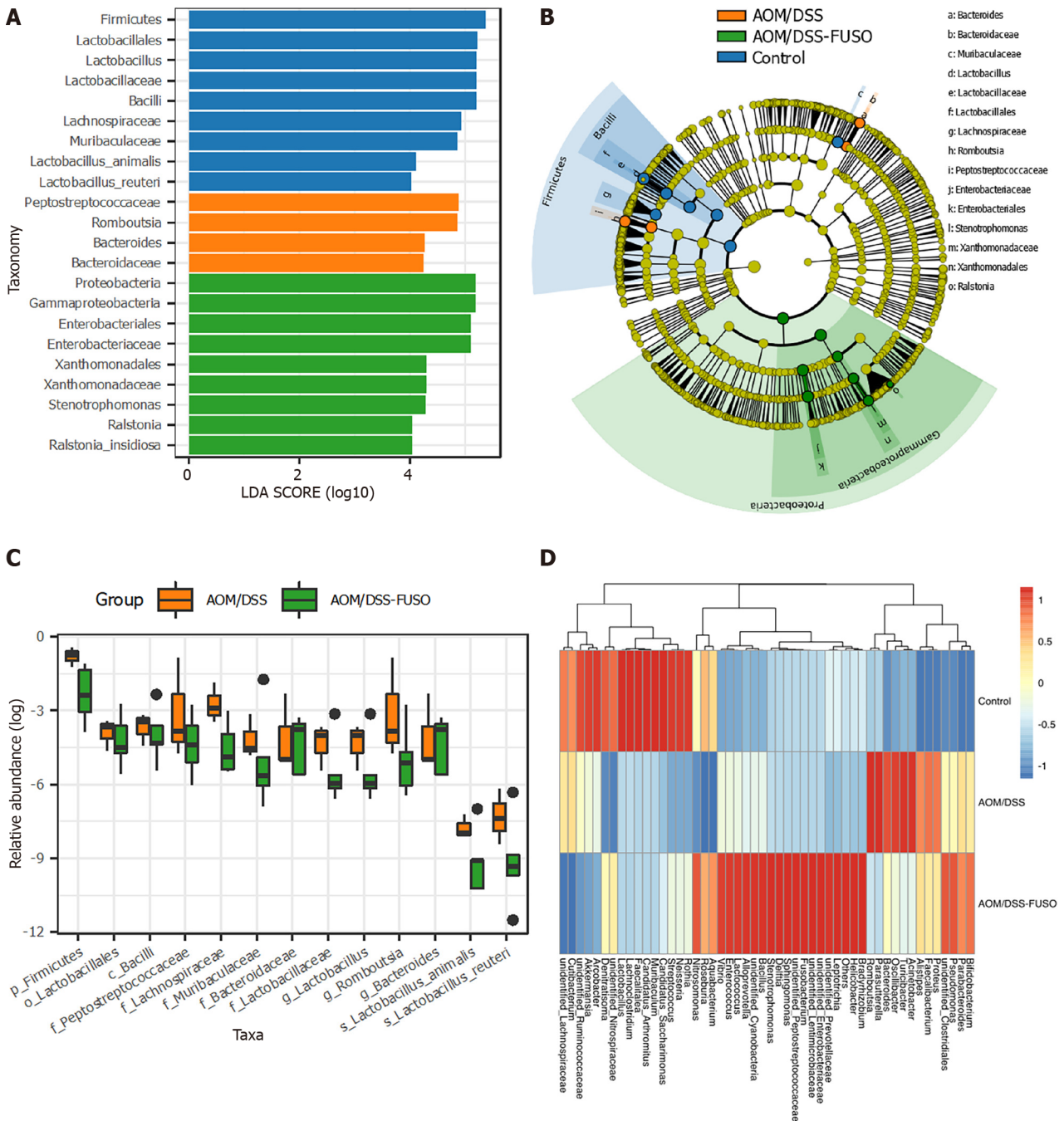
To gain insights into the molecular basis underlying the protumorigenic effect of *Fusobacterium* infection, RNA-seq was performed to reveal the transcriptomic changes driven by *F. nucleatum*. We observed different number of DEGs in the three comparions, *i.e.*, AOM/DSS *vs* Control, AOM/DSS-FUSO *vs* Control, and AOM/DSS-FUSO *vs* AOM/DSS (Figure 4A-C), and compared with the

Figure 2 Diversity and shared operational taxonomic units of the gut microbiota in different groups. A: Nonmetric multidimensional plot of the cecal microbiota from the 14 samples based on Bray-Curtis similarities; B: Principal coordinate analysis plot of the cecal microbiota from the 14 samples based on Bray-Curtis similarities; C: Weighted UniFrac distance of the samples from different groups. Kruskal-Wallis test: $P = 6.12 \times 10^{-7}$; D: Number of shared operational taxonomic units between the samples from the azoxymethane-dextran sulfate sodium salt (AOM/DSS)-FUSO group and the AOM/DSS group. AOM: Azoxymethane; DSS: Dextran sulfate sodium salt.

AOM/DSS mice, there were 231 upregulated genes and 92 downregulated genes in the AOM/DSS-FUSO mice (Figure 4C). The heatmap of DEGs showed the distinct gene expression profile between AOM/DSS-induced CRC models with or without overloaded *F. nucleatum* treatment (Figure 4D). These upregulated genes included FABP1 (fatty acid binding protein 1)[34], sucrase isomaltase, defensin, ATP-binding cassette[35], homeobox C6[36] and tolloid-like 2 (NETO2)[37], all of which were overexpressed more than 3-fold and were correlated with a poor prognosis of colorectal carcinoma in previous studies (Supplementary Table 1). KEGG pathway enrichment analysis suggested that the microbiota-transcriptome interaction significantly upregulated neuroactive ligand–receptor interaction, cyclic adenosine monophosphate (cAMP) signaling pathway, PPAR signaling pathway, steroid hormone biosynthesis, retinol metabolism, mineral absorption and drug metabolism in the AOM/DSS-FUSO group (Figure 5), and 36 DEGs were included in these KEGG pathways (Supplementary Figure 4). Among them, several CRC-related DEGs, PPARα[38], PCK1[39,40], GCG[41], VAV2[42], and ANGPTL4 [43] were also revealed to be correlated with the CRC prognosis in previous studies. These results

Figure 3 The differentially abundant taxa among the three groups. A: Histogram of the linear discriminant analysis scores computed for taxa that were differentially abundant among the three groups; B: Taxonomic representation of statistically and biologically consistent differences among the three groups. The differences are represented in the color of the most abundant class; C: Relative abundance of the taxa in azoxymethane/dextran sulfate sodium salt (AOM/DSS)-FUSO and AOM/DSS; D: Patterns of the abundance of the top 50 operational taxonomic units in all samples. The colors indicate the Z scores of the mean abundance in each group. AOM: Azoxymethane; DSS: Dextran sulfate sodium salt.

suggested that dramatic changes occurred in the host signaling pathways that are related to the tumori-genesis of CRC after *F. nucleatum* infection and the resulting disturbance of the mucosal microbiota.

Hub bacteria and key genes involved in the carcinogenesis/development of CRC
To further explore the hub bacteria and the hub DEGs, MCODE plugged in Cytoscape was used to explore the key modules involved in CRC development (Figure 6). The differential bacterial taxa identified by LEfSe analysis and the genes involved in the top seven significantly differential KEGG pathways were processed. The results showed that seven potentially harmful hub taxa were closely related to the overexpression of 12 hub genes. These taxa, *Stenotrophomonas*[44], Xanthomonadaceae, Xanthomonadales, Enterobacteriaceae, Enterobacteriales, Gammaproteobacteria, and Proteobacteria, have been shown to exhibit proinflammatory and procarcinogenic properties. This key module with the
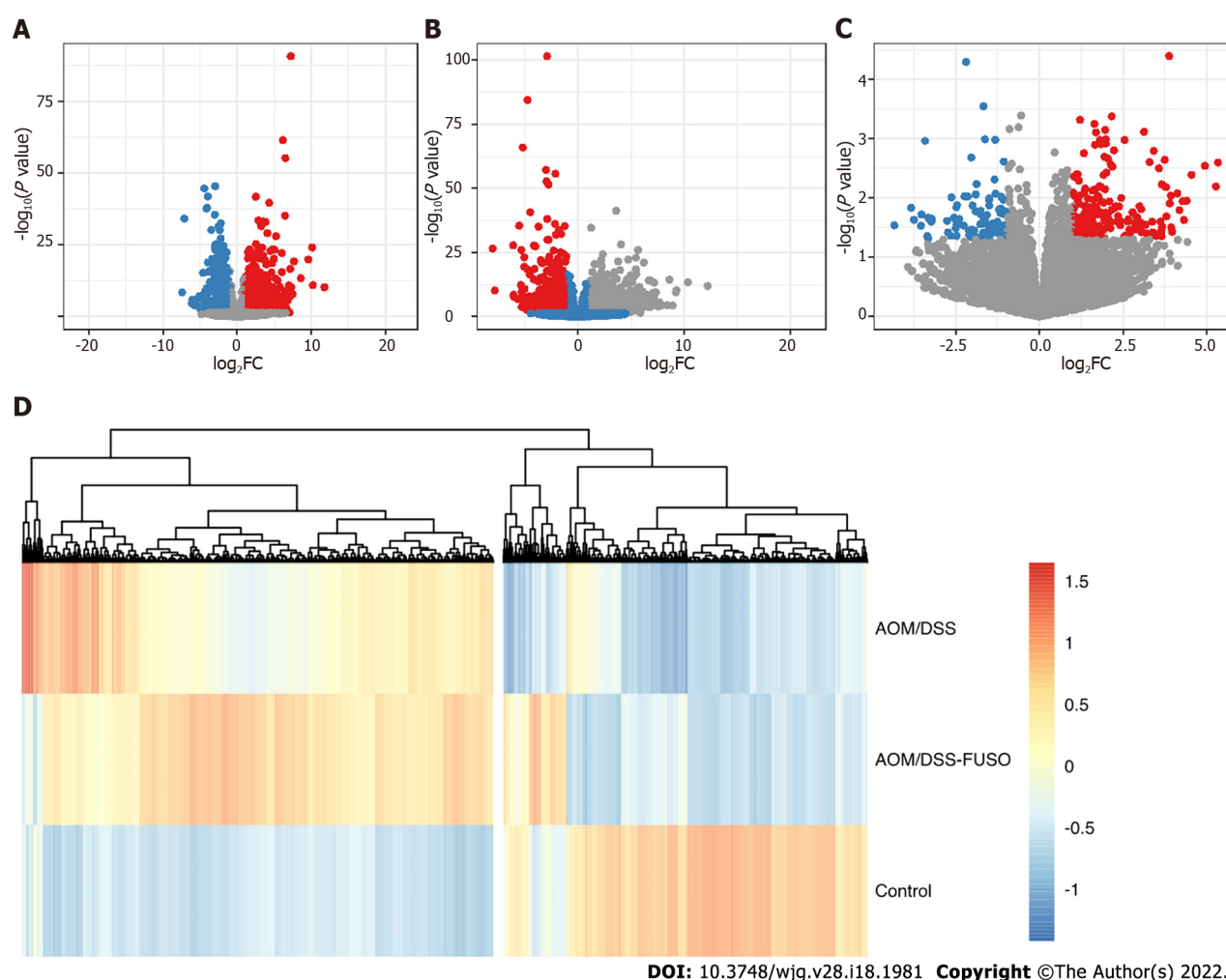
Figure 4 The differentially expressed genes of the mucosa. A: Volcano plot showing the differentially expressed genes between the azoxymethane/dextran sulfate sodium salt (AOM/DSS) group and the control group; B: Volcano plot showing the differentially expressed genes between the AOM/DSS-FUSO group and the control group; C: Volcano plot showing the differentially expressed genes between the AOM/DSS-FUSO group and the AOM/DSS group. Significantly upregulated genes are shown in red ($P < 0.05$ and $\log_2FC \geq 1$). Significantly downregulated genes are shown in blue ($P < 0.05$ and $\log_2FC \leq -1$). The numbers of significantly upregulated genes were 1374 for (A), 1939 for (B) and 231 for (C). The numbers of significantly downregulated genes were 1050 for (A), 1104 for (B) and 92 for (C); D: Patterns of the abundance of all of the differentially expressed genes in the upper panels. The colors indicate the Z scores of the mean abundance in each group. AOM: Azoxymethane; DSS: Dextran sulfate sodium salt.

seven hub microbial taxa and 12 hub genes may regulate the occurrence and development of CRC through CRC-related pathways such as the cAMP and PPAR signaling pathways. Enterobacteriaceae correlated with eight oncogenes, *i.e.*, *PCK1*, *GalR2*, *GCG*, *SLC6A19*, *CHRM1*, *ADRB1*, *UGT2B38*, and *GRID2*, and three taxa (Xanthomonadales, Xanthomonadaceae and *Stenotrophomonas*) were positively correlated with *VAV2*, *SCTR* and *ANGPTL4*. These results suggested that the dysbiosis of gut microbes driven by *F. nucleatum* infection may have the potential to affect the transcriptional activity of tumor-related metabolic pathways, especially those containing oncogenes.

DISCUSSION

F. nucleatum has long been known to cause opportunistic infections and has recently been implicated in CRC, which has attracted broad attention. Previously, we found that the RA of *F. nucleatum* in the fecal microbiota was significantly increased in CRC patients[33]. However, the effect of *F. nucleatum* infection on the mucosal microbiota and the resulting relationship between gut microbiome alterations and CRC development are still open questions. AOM/DSS mice can spontaneously develop multiple intestinal adenomas and have been used extensively as a model of colorectal carcinogenesis inflammation-associated tumors[45]. We showed that AOM/DSS mice with *F. nucleatum* infection have a higher burden of intestinal adenoma and worse colon histology. At the same time, an impaired mucosal barrier as shown by E-cadherin expression and increased epithelial cell proliferation by Ki-67 in the AOM/DSS-FUSO group were observed.
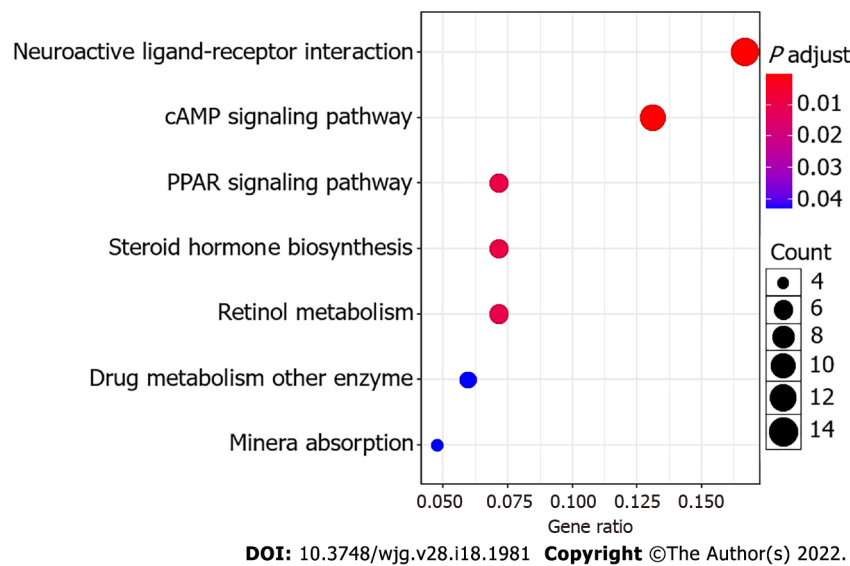
DOI: 10.3748/wjg.v28.i18.1981 **Copyright** ©The Author(s) 2022.

Figure 5 Bubble plot of the KEGG pathways. The size of the bubble indicates the relative number of genes in the set. The color of the bubble indicates the adjusted *P* value.
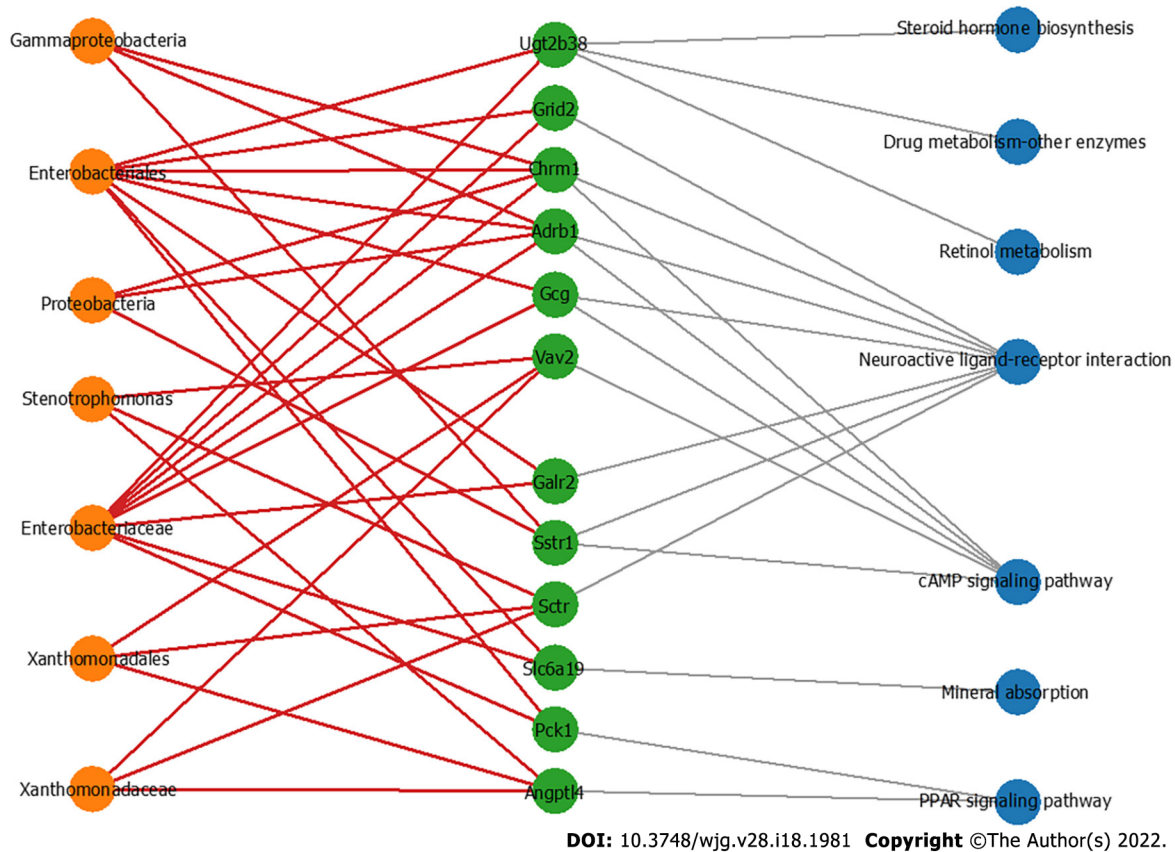

DOI: 10.3748/wjg.v28.i18.1981 **Copyright** ©The Author(s) 2022.

Figure 6 The co-occurrence network shows the correlations of the colon mucosa microbiota with the differentially expressed genes.
Edges: Correlations with *P* values < 0.01; red edges: Positive correlations; gray edges: Relationship between the genes and the pathways; green nodes: Genes involved in the top seven significantly differential KEGG pathways in the azoxymethane/dextran sulfate sodium salt (AOM/DSS)-FUSO group compared with the AOM/DSS group; orange nodes: The differential bacterial taxa identified by LEfSe analysis; blue nodes: Related pathways of defferentially expressed genes.

After the introduction of *F. nucleatum*, we propose that *F. nucleatum* needs to adapt to and change the symbiotic microbial environment, which could activate and promote the progression of colorectal carcinogenesis. In this study, three increased inflammation-inducing bacteria and three decreased probiotic genera in the top 50 differentially expressed genera were recognized as dysbiotic mucosal taxa after *F. nucleatum* stimulation. Furthermore, changes in the structure of the mucosal microbiota among the three groups were identified. Proteobacteria and eight other pathogenic bacterial taxa (Figure 3A)

were the dominant taxa in the AOM/DSS-FUSO mice compared with the AOM/DSS group. In agreement with previous studies, gut microbial comparisons of CRC patients and non-CRC subjects are characterized by a high prevalence of pro-inflammatory bacteria (mostly Proteobacteria) and a decrease in commensal beneficial bacteria (mostly Firmicutes)[33,46,47]. Notably, the transfer of two Enterobacteriaceae species (*Klebsiella pneumoniae* and *Proteus mirabilis*) was sufficient to provoke colitis in the recipient mice[48]. The overload of Proteobacteria promoted intestinal inflammation in a T-bet^{-/-} Rag2^{-/-} mouse model of colitis[48-50]. Similar to studies in mice, microbiota studies in humans have shown that the gut microbial structure of inflammatory bowel disease patients is characterized by an expansion of Proteobacteria, particularly Enterobacteriaceae. Consistent with previous studies, we observed that the RA of Enterobacteriaceae in the mucosal microbiota was positively correlated with the expression of key oncogenes. Moreover, three other taxa, *Stenotrophomonas*, Xanthomonadales, and Xanthomonadaceae, were positively correlated with ATGPTL4 (angiopoietin-like 4), the VAV2 oncogene, and SCTR (secretin receptor), as shown in Figure 6. *Stenotrophomonas* was proven to be significantly increased during the exacerbated phase of UC compared to the remission phase[51]. Based on the above evidence, we propose that abnormal expansion of Proteobacteria, especially Enterobacteriaceae and *Stenotrophomonas*, is the signature of microbial dysbiosis driven by *F. nucleatum*.

To further reveal the effects of *F. nucleatum* infection and microbial dysbiosis on the transcriptome of AOM/DSS mice, RNA-seq was performed, and 323 DEGs were identified that were influenced by the oncogenic microbial environment. Interestingly, we found that the *F. nucleatum*-driven DEGs were significantly enriched in cancer-related KEGG signaling pathways. The neuroactive ligand–receptor interaction, cAMP signaling pathway, and PPAR signaling pathway were significantly overexpressed in the AOM/DSS-FUSO group. Among them, ANGPTL4, VAV2, and PCK1 were significantly highly expressed in the AOM/DSS-FUSO groups and positively correlated with the Proteobacteria taxa. In CRC cell lines, Zheng *et al*[52] found that *F. nucleatum* infection provoked glucose uptake and subsequently promoted glycolysis activity of CRC cells *via* ATGPTL4, which could in turn facilitate its own colonization in CRC cells[52]. *F. nucleatum*-mediated glycolysis activation *via* ATGPTL4 plays important roles in the pathogenesis of CRC and subsequently provides a beneficial environment for the outgrowth of CRC-related taxa.

Consistent with our results, other recent studies have demonstrated that *F. nucleatum* provokes glycolysis by upregulating lncRNA ENO-1[53], and an increase in cellular metabolic activity provides ample cellular energy for EMT-mediated metastasis[54]. Another oncogene, *VAV2*, related to three Proteobacteria taxa, is a member of the VAV guanine nucleotide exchange factor family of oncogenes and is one of the five combined prognostic genes that was identified to form a prognostic mutation panel for predicting cancer recurrence in stage II and III CRC[55]. Loss of VAV2, VAV3 and TIAM1 is sufficient to strongly suppress the cancer phenotypes and tumorigenesis induced by APC loss[56].

It is important to note that the eight upregulated hub genes shown in the microbiota-transcriptome network were positively correlated with high levels of Enterobacteriaceae, *e.g.*, PCK1, GalR2, GCG, SLC6A19, CHRM1, ADRB1, UGT2B38, and GRID2. Among them, PCK1 enhanced liver metastatic growth by driving pyrimidine nucleotide biosynthesis under hypoxia[40]. G-protein-coupled receptor galanin receptor 1 (GalR1) was identified as a novel regulator of drug resistance[57]. Notably, silencing either GalR1 or its ligand, galanin, induced apoptosis in both drug-sensitive and drug-resistant cell lines and synergistically enhanced the effects of chemotherapy. Mechanistically, GalR1/galanin silencing resulted in downregulation of the endogenous caspase-8 inhibitor FLIP(L), resulting in induction of caspase-8-dependent apoptosis. *Galanin* mRNA was found to be overexpressed in colorectal tumors, and importantly, high galanin expression was correlated with poor disease-free survival of patients with early-stage CRC. In the future, additional studies need to be performed to explore the effect of *F. nucleatum* on Proteobacteria-related oncogenes to clarify the roles of *F. nucleatum* in CRC diseases.

Therefore, our data present the key microbial signature after *F. nucleatum* infection, which may provide new insights into the role of dysbiosis in the mucosal microbiota driven by *F. nucleatum* in promoting CRC. We provide direct evidence that Proteobacteria expansion, in particular Enterobacteriaceae and *Stenotrophomonas*, occurs during *F. nucleatum* infection, leading to the differential expression of oncogene transcriptomes in the AOM/DSS model. We provide evidence that *F. nucleatum* interacts with other species, how it remodels the microbiota, and how it alters the tumor microenvironment. Furthermore, we revealed the dysbiosis signature of the colon mucosa microbiota driven by *Fusobacterium* and the interaction between the hub microbial taxa and the host transcriptome. A deeper understanding of CRC etiology will also help identify new targets for prevention and treatment.

CONCLUSION

In conclusion, these data extend our previous work to provide evidence for microbial dysbiosis in CRC and suggest the existence of a defined set of microbiota whose composition is essential. Our study is also distinct in taking a holistic approach, given the observation of important bacterial-host networks and evidence for an oncogenic microbial environment of the colon promoting the formation of CRC. Our study is limited by: (1) The lack of time-course experiments to validate the effects of *F. nucleatum* on

the symbiotic microenvironment; and (2) The limited sample size due to the deaths of mice when establishing the disease model. Therefore, further studies using more mice to establish the disease model are required to confirm the findings here and to disentangle the defined role of the Proteobacteria-related oncogenes driven by *F. nucleatum* during the progression of colorectal adenomas.

ARTICLE HIGHLIGHTS

Research background
Fusobacterium nucleatum (*F. nucleatum*) has long been known to cause opportunistic infections and has recently been implicated in colorectal cancer (CRC), which has attracted broad attention. Exploring the roles and underlying mechanism of *F. nucleatum* has important theoretical and practical significance for diagnosis and targeted therapy of CRC.

Research motivation
The aim of this study is to reveal the effect of *F. nucleatum* infection on the changes of mucosal microbiota, and investigate the regulatory role of *F. nucleatum* in the CRC progression.

Research objectives
The azoxymethane/dextran sulfate sodium salt (AOM/DSS)-induced mice were used to investigate the role of *F. nucleatum* in the "oncogenic microbial environment" of the colon.

Research methods
The mucosal microbial composition and RNA-seq transcriptomic analysis were used to identify the differentially expressed gene (DEG) signatures driven by *F. nucleatum* infection, and integrated network analysis was conducted to reveal the relationship between microbial dysbiosis and the DEGs.

Research results
We provide direct evidence that *F. nucleatum* interacts with other species, remodels the microbiota, and alters the tumor microenvironment. In addition, we revealed the dysbiosis signature of the colon mucosa microbiota driven by *F. nucleatum* and the interaction between the hub microbial taxa and the host transcriptome.

Research conclusions
Dysbiosis in the mucosal microbiota driven by *F. nucleatum*, in particular Enterobacteriaceae and *Stenotrophomonas*, occurs during *F. nucleatum* infection, leading to the differential expression of oncogene transcriptomes in the AOM/DSS model.

Research perspectives
Our study provides a deeper insight into CRC etiology driven by *F. nucleatum* infection and the mechanisms of the tumorigenic effect of *F. nucleatum*. Targeting *F. nucleatum* infection is a potential treatment for CRC.

FOOTNOTES

revised according to the ARRIVE guidelines.

Open-Access: This article is an open-access article that was selected by an in-house editor and fully peer-reviewed by external reviewers. It is distributed in accordance with the Creative Commons Attribution NonCommercial (CC BY-NC 4.0) license, which permits others to distribute, remix, adapt, build upon this work non-commercially, and license their derivative works on different terms, provided the original work is properly cited and the use is non-commercial. See: https://creativecommons.org/Licenses/by-nc/4.0/

Country/Territory of origin: China

ORCID number: Na Wu 0000-0001-6803-8337; Yu-Qing Feng 0000-0002-7742-5272; Na Lyu 0000-0003-0603-6170; Di Wang 0000-0003-0553-7977; Wei-Dong Yu 0000-0002-7573-4979; Yong-Fei Hu 0000-0002-2158-6018.

REFERENCES

1   **Song M**, Garrett WS, Chan AT. Nutrients, foods, and colorectal cancer prevention. *Gastroenterology* 2015; **148**: 1244-60.e16 [PMID: 25575572 DOI: 10.1053/j.gastro.2014.12.035]

2   **Chen W**, Zheng R, Baade PD, Zhang S, Zeng H, Bray F, Jemal A, Yu XQ, He J. Cancer statistics in China, 2015. *CA Cancer J Clin* 2016; **66**: 115-132 [PMID: 26808342 DOI: 10.3322/caac.21338]

3   **Kostic AD**, Chun E, Robertson L, Glickman JN, Gallini CA, Michaud M, Clancy TE, Chung DC, Lochhead P, Hold GL, El-Omar EM, Brenner D, Fuchs CS, Meyerson M, Garrett WS. *Fusobacterium nucleatum* potentiates intestinal tumorigenesis and modulates the tumor-immune microenvironment. *Cell Host Microbe* 2013; **14**: 207-215 [PMID: 23954159 DOI: 10.1016/j.chom.2013.07.007]

4   **Castellarin M**, Warren RL, Freeman JD, Dreolini L, Krzywinski M, Strauss J, Barnes R, Watson P, Allen-Vercoe E, Moore RA, Holt RA. *Fusobacterium nucleatum* infection is prevalent in human colorectal carcinoma. *Genome Res* 2012; **22**: 299-306 [PMID: 22009989 DOI: 10.1101/gr.126516.111]

5   **Li YY**, Ge QX, Cao J, Zhou YJ, Du YL, Shen B, Wan YJ, Nie YQ. Association of *Fusobacterium nucleatum* infection with colorectal cancer in Chinese patients. *World J Gastroenterol* 2016; **22**: 3227-3233 [PMID: 27004000 DOI: 10.3748/wjg.v22.i11.3227]

6   **Mima K**, Nishihara R, Qian ZR, Cao Y, Sukawa Y, Nowak JA, Yang J, Dou R, Masugi Y, Song M, Kostic AD, Giannakis M, Bullman S, Milner DA, Baba H, Giovannucci EL, Garraway LA, Freeman GJ, Dranoff G, Garrett WS, Huttenhower C, Meyerson M, Meyerhardt JA, Chan AT, Fuchs CS, Ogino S. *Fusobacterium nucleatum* in colorectal carcinoma tissue and patient prognosis. *Gut* 2016; **65**: 1973-1980 [PMID: 26311717 DOI: 10.1136/gutjnl-2015-310101]

7   **Xu M**, Yamada M, Li M, Liu H, Chen SG, Han YW. FadA from *Fusobacterium nucleatum* utilizes both secreted and nonsecreted forms for functional oligomerization for attachment and invasion of host cells. *J Biol Chem* 2007; **282**: 25000-25009 [PMID: 17588948 DOI: 10.1074/jbc.M611567200]

8   **Fardini Y**, Wang X, Témoin S, Nithianantham S, Lee D, Shoham M, Han YW. *Fusobacterium nucleatum* adhesin FadA binds vascular endothelial cadherin and alters endothelial integrity. *Mol Microbiol* 2011; **82**: 1468-1480 [PMID: 22040113 DOI: 10.1111/j.1365-2958.2011.07905.x]

9   **Yang Y**, Weng W, Peng J, Hong L, Yang L, Toiyama Y, Gao R, Liu M, Yin M, Pan C, Li H, Guo B, Zhu Q, Wei Q, Moyer MP, Wang P, Cai S, Goel A, Qin H, Ma Y. *Fusobacterium nucleatum* increases proliferation of colorectal cancer cells and tumor development in mice by activating Toll-like receptor 4 signaling to nuclear factor-κB, and up-regulating expression of microRNA-21. *Gastroenterology* 2017; **152**: 851-866.e24 [PMID: 27876571 DOI: 10.1053/j.gastro.2016.11.018]

10   **Abed J**, Emgård JE, Zamir G, Faroja M, Almogy G, Grenov A, Sol A, Naor R, Pikarsky E, Atlan KA, Mellul A, Chaushu S, Manson AL, Earl AM, Ou N, Brennan CA, Garrett WS, Bachrach G. Fap2 mediates *Fusobacterium nucleatum* colorectal adenocarcinoma enrichment by binding to tumor-expressed Gal-GalNAc. *Cell Host Microbe* 2016; **20**: 215-225 [PMID: 27512904 DOI: 10.1016/j.chom.2016.07.006]

11   **Kang W**, Sun T, Tang D, Zhou J, Feng Q. Time-course transcriptome analysis of gingiva-derived mesenchymal stem cells reveals that *Fusobacterium nucleatum* triggers oncogene expression in the process of cell differentiation. *Front Cell Dev Biol* 2019; **7**: 359 [PMID: 31993418 DOI: 10.3389/fcell.2019.00359]

12   **Wang L**, Peng F, Peng C, Du JR. Gut microbiota in tumor microenvironment: A critical regulator in cancer initiation and development as potential targets for Chinese medicine. *Am J Chin Med* 2021; **49**: 609-626 [PMID: 33683187 DOI: 10.1142/S0192415X21500270]

13   **Wong-Rolle A**, Wei HK, Zhao C, Jin C. Unexpected guests in the tumor microenvironment: microbiome in cancer. *Protein Cell* 2021; **12**: 426-435 [PMID: 33296049 DOI: 10.1007/s13238-020-00813-8]

14   **Garrett WS**. Cancer and the microbiota. *Science* 2015; **348**: 80-86 [PMID: 25838377 DOI: 10.1126/science.aaa4972]

15   **Doulberis M**, Angelopoulou K, Kaldrymidou E, Tsingotjidou A, Abas Z, Erdman SE, Poutahidis T. Cholera-toxin suppresses carcinogenesis in a mouse model of inflammation-driven sporadic colon cancer. *Carcinogenesis* 2015; **36**: 280-290 [PMID: 25550315 DOI: 10.1093/carcin/bgu325]

16   **Liu L**, Liang L, Liang H, Wang M, Lu B, Xue M, Deng J, Chen Y. *Fusobacterium nucleatum* aggravates the progression of colitis by regulating M1 macrophage polarization *via* AKT2 pathway. *Front Immunol* 2019; **10**: 1324 [PMID: 31249571

DOI: 10.3389/fimmu.2019.01324]

17   **Yu Y**, Lee C, Kim J, Hwang S. Group-specific primer and probe sets to detect methanogenic communities using quantitative real-time polymerase chain reaction. *Biotechnol Bioeng* 2005; **89**: 670-679 [PMID: 15696537 DOI: 10.1002/bit.20347]

18   **Chen S**, Zhou Y, Chen Y, Gu J. fastp: An ultra-fast all-in-one FASTQ preprocessor. *Bioinformatics* 2018; **34**: i884-i890 [PMID: 30423086 DOI: 10.1093/bioinformatics/bty560]

19   **Rognes T**, Flouri T, Nichols B, Quince C, Mahé F. VSEARCH: A versatile open source tool for metagenomics. *PeerJ* 2016; **4**: e2584 [PMID: 27781170 DOI: 10.7717/peerj.2584]

20   **Edgar RC**. UPARSE: highly accurate OTU sequences from microbial amplicon reads. *Nat Methods* 2013; **10**: 996-998 [PMID: 23955772 DOI: 10.1038/nmeth.2604]

21   **Schloss PD**. A high-throughput DNA sequence aligner for microbial ecology studies. *PLoS One* 2009; **4**: e8230 [PMID: 20011594 DOI: 10.1371/journal.pone.0008230]

22   **Caporaso JG**, Kuczynski J, Stombaugh J, Bittinger K, Bushman FD, Costello EK, Fierer N, Peña AG, Goodrich JK, Gordon JI, Huttley GA, Kelley ST, Knights D, Koenig JE, Ley RE, Lozupone CA, McDonald D, Muegge BD, Pirrung M, Reeder J, Sevinsky JR, Turnbaugh PJ, Walters WA, Widmann J, Yatsunenko T, Zaneveld J, Knight R. QIIME allows analysis of high-throughput community sequencing data. *Nat Methods* 2010; **7**: 335-336 [PMID: 20383131 DOI: 10.1038/nmeth.f.303]

23   **Lozupone C**, Knight R. UniFrac: A new phylogenetic method for comparing microbial communities. *Appl Environ Microbiol* 2005; **71**: 8228-8235 [PMID: 16332807 DOI: 10.1128/AEM.71.12.8228-8235.2005]

24   **Kim D**, Langmead B, Salzberg SL. HISAT: A fast spliced aligner with low memory requirements. *Nat Methods* 2015; **12**: 357-360 [PMID: 25751142 DOI: 10.1038/nmeth.3317]

25   **Liao Y**, Smyth GK, Shi W. featureCounts: An efficient general purpose program for assigning sequence reads to genomic features. *Bioinformatics* 2014; **30**: 923-930 [PMID: 24227677 DOI: 10.1093/bioinformatics/btt656]

26   **Klipper-Aurbach Y**, Wasserman M, Braunspiegel-Weintrob N, Borstein D, Peleg S, Assa S, Karp M, Benjamini Y, Hochberg Y, Laron Z. Mathematical formulae for the prediction of the residual beta cell function during the first two years of disease in children and adolescents with insulin-dependent diabetes mellitus. *Med Hypotheses* 1995; **45**: 486-490 [PMID: 8748093 DOI: 10.1016/0306-9877(95)90228-7]

27   **Wu T**, Hu E, Xu S, Chen M, Guo P, Dai Z, Feng T, Zhou L, Tang W, Zhan L, Fu X, Liu S, Bo X, Yu G. clusterProfiler 4.0: A universal enrichment tool for interpreting omics data. *Innovation (N Y)* 2021; **2**: 100141 [PMID: 34557778 DOI: 10.1016/j.xinn.2021.100141]

28   **Zapala MA**, Schork NJ. Multivariate regression analysis of distance matrices for testing associations between gene expression patterns and related variables. *Proc Natl Acad Sci U S A* 2006; **103**: 19430-19435 [PMID: 17146048 DOI: 10.1073/pnas.0609333103]

29   **Segata N**, Izard J, Waldron L, Gevers D, Miropolsky L, Garrett WS, Huttenhower C. Metagenomic biomarker discovery and explanation. *Genome Biol* 2011; **12**: R60 [PMID: 21702898 DOI: 10.1186/gb-2011-12-6-r60]

30   **Shannon P**, Markiel A, Ozier O, Baliga NS, Wang JT, Ramage D, Amin N, Schwikowski B, Ideker T. Cytoscape: A software environment for integrated models of biomolecular interaction networks. *Genome Res* 2003; **13**: 2498-2504 [PMID: 14597658 DOI: 10.1101/gr.1239303]

31   **Neufert C**, Heichler C, Brabletz T, Scheibe K, Boonsanay V, Greten FR, Neurath MF. Inducible mouse models of colon cancer for the analysis of sporadic and inflammation-driven tumor progression and lymph node metastasis. *Nat Protoc* 2021; **16**: 61-85 [PMID: 33318692 DOI: 10.1038/s41596-020-00412-1]

32   **Stemmler MP**, Eccles RL, Brabletz S, Brabletz T. Non-redundant functions of EMT transcription factors. *Nat Cell Biol* 2019; **21**: 102-112 [PMID: 30602760 DOI: 10.1038/s41556-018-0196-y]

33   **Wu N**, Yang X, Zhang R, Li J, Xiao X, Hu Y, Chen Y, Yang F, Lu N, Wang Z, Luan C, Liu Y, Wang B, Xiang C, Wang Y, Zhao F, Gao GF, Wang S, Li L, Zhang H, Zhu B. Dysbiosis signature of fecal microbiota in colorectal cancer patients. *Microb Ecol* 2013; **66**: 462-470 [PMID: 23733170 DOI: 10.1007/s00248-013-0245-9]

34   **Zhang Y**, Zhang W, Xia M, Xie Z, An F, Zhan Q, Tian W, Zhu T. High expression of FABP4 in colorectal cancer and its clinical significance. *J Zhejiang Univ Sci B* 2021; **22**: 136-145 [PMID: 33615754 DOI: 10.1631/jzus.B2000366]

35   **Zhang Q**, Zhao H, Wu D, Cao D, Ma W. A comprehensive analysis of the microbiota composition and gene expression in colorectal cancer. *BMC Microbiol* 2020; **20**: 308 [PMID: 33050883 DOI: 10.1186/s12866-020-01938-w]

36   **Ji M**, Feng Q, He G, Yang L, Tang W, Lao X, Zhu D, Lin Q, Xu P, Wei Y, Xu J. Silencing homeobox C6 inhibits colorectal cancer cell proliferation. *Oncotarget* 2016; **7**: 29216-29227 [PMID: 27081081 DOI: 10.18632/oncotarget.8703]

37   **Hu L**, Chen HY, Cai J, Yang GZ, Feng D, Zhai YX, Gong H, Qi CY, Zhang Y, Fu H, Cai QP, Gao CF. Upregulation of NETO2 expression correlates with tumor progression and poor prognosis in colorectal carcinoma. *BMC Cancer* 2015; **15**: 1006 [PMID: 26699544 DOI: 10.1186/s12885-015-2018-y]

38   **Chang H**, Zhao F, Xie X, Liao Y, Song Y, Liu C, Wu Y, Wang Y, Liu D, Zou J, Qi Z. PPARα suppresses Th17 cell differentiation through IL-6/STAT3/RORγt pathway in experimental autoimmune myocarditis. *Exp Cell Res* 2019; **375**: 22-30 [PMID: 30557558 DOI: 10.1016/j.yexcr.2018.12.005]

39   **Yang J**, Gao S, Qiu M, Kan S. Integrated Analysis of Gene Expression and metabolite data reveals candidate molecular markers in colorectal carcinoma. *Cancer Biother Radiopharm* 2020 [PMID: 33259728 DOI: 10.1089/cbr.2020.3980]

40   **Yamaguchi N**, Weinberg EM, Nguyen A, Liberti MV, Goodarzi H, Janjigian YY, Paty PB, Saltz LB, Kingham TP, Loo JM, de Stanchina E, Tavazoie SF. PCK1 and DHODH drive colorectal cancer liver metastatic colonization and hypoxic growth by promoting nucleotide synthesis. *Elife* 2019; **8**: e52135 [PMID: 31841108 DOI: 10.7554/eLife.52135]

41   **Bian Q**, Chen J, Qiu W, Peng C, Song M, Sun X, Liu Y, Ding F, Zhang L. Four targeted genes for predicting the prognosis of colorectal cancer: A bioinformatics analysis case. *Oncol Lett* 2019; **18**: 5043-5054 [PMID: 31612015 DOI: 10.3892/ol.2019.10866]

42   **Hebeis B**, Vigorito E, Kovesdi D, Turner M. Vav proteins are required for B-lymphocyte responses to LPS. *Blood* 2005; **106**: 635-640 [PMID: 15811961 DOI: 10.1182/blood-2004-10-3919]

43   **Wen L**, Zhang Y, Yang B, Han F, Ebadi AG, Toughani M. Knockdown of Angiopoietin-like protein 4 suppresses the

development of colorectal cancer. *Cell Mol Biol (Noisy-le-grand)* 2020; **66**: 117-124 [PMID: 33040824 DOI: 10.3892/or.2018.6253]

44 **Merlo LMF**, DuHadaway JB, Montgomery JD, Peng WD, Murray PJ, Prendergast GC, Caton AJ, Muller AJ, Mandik-Nayak L. Differential roles of IDO1 and IDO2 in T and B cell inflammatory immune responses. *Front Immunol* 2020; **11**: 1861 [PMID: 32973768 DOI: 10.3389/fimmu.2020.01861]

45 **Neufert C**, Becker C, Neurath MF. An inducible mouse model of colon carcinogenesis for the analysis of sporadic and inflammation-driven tumor progression. *Nat Protoc* 2007; **2**: 1998-2004 [PMID: 17703211 DOI: 10.1038/nprot.2007.279]

46 **Chamorro N**, Montero DA, Gallardo P, Farfán M, Contreras M, De la Fuente M, Dubois K, Hermoso MA, Quera R, Pizarro-Guajardo M, Paredes-Sabja D, Ginard D, Rosselló-Móra R, Vidal R. Landscapes and bacterial signatures of mucosa-associated intestinal microbiota in Chilean and Spanish patients with inflammatory bowel disease. *Microb Cell* 2021; **8**: 223-238 [PMID: 34527721 DOI: 10.15698/mic2021.09.760]

47 **Wassenaar TM**. E. coli and colorectal cancer: A complex relationship that deserves a critical mindset. *Crit Rev Microbiol* 2018; **44**: 619-632 [PMID: 29909724 DOI: 10.1080/1040841X.2018.1481013]

48 **Garrett WS**, Gallini CA, Yatsunenko T, Michaud M, DuBois A, Delaney ML, Punit S, Karlsson M, Bry L, Glickman JN, Gordon JI, Onderdonk AB, Glimcher LH. Enterobacteriaceae act in concert with the gut microbiota to induce spontaneous and maternally transmitted colitis. *Cell Host Microbe* 2010; **8**: 292-300 [PMID: 20833380 DOI: 10.1016/j.chom.2010.08.004]

49 **Shin NR**, Whon TW, Bae JW. Proteobacteria: microbial signature of dysbiosis in gut microbiota. *Trends Biotechnol* 2015; **33**: 496-503 [PMID: 26210164 DOI: 10.1016/j.tibtech.2015.06.011]

50 **Rooks MG**, Veiga P, Wardwell-Scott LH, Tickle T, Segata N, Michaud M, Gallini CA, Beal C, van Hylckama-Vlieg JE, Ballal SA, Morgan XC, Glickman JN, Gevers D, Huttenhower C, Garrett WS. Gut microbiome composition and function in experimental colitis during active disease and treatment-induced remission. *ISME J* 2014; **8**: 1403-1417 [PMID: 24500617 DOI: 10.1038/ismej.2014.3]

51 **Walujkar SA**, Kumbhare SV, Marathe NP, Patangia DV, Lawate PS, Bharadwaj RS, Shouche YS. Molecular profiling of mucosal tissue associated microbiota in patients manifesting acute exacerbations and remission stage of ulcerative colitis. *World J Microbiol Biotechnol* 2018; **34**: 76 [PMID: 29796862 DOI: 10.1007/s11274-018-2449-0]

52 **Zheng X**, Liu R, Zhou C, Yu H, Luo W, Zhu J, Liu J, Zhang Z, Xie N, Peng X, Xu X, Cheng L, Yuan Q, Huang C, Zhou X. ANGPTL4-mediated promotion of glycolysis facilitates the colonization of *Fusobacterium nucleatum* in colorectal cancer. *Cancer Res* 2021; **81**: 6157-6170 [PMID: 34645607 DOI: 10.1158/0008-5472.CAN-21-2273]

53 **Hong J**, Guo F, Lu SY, Shen C, Ma D, Zhang X, Xie Y, Yan T, Yu T, Sun T, Qian Y, Zhong M, Chen J, Peng Y, Wang C, Zhou X, Liu J, Liu Q, Ma X, Chen YX, Chen H, Fang JY. *F. nucleatum* targets lncRNA ENO1-IT1 to promote glycolysis and oncogenesis in colorectal cancer. *Gut* 2021; **70**: 2123-2137 [PMID: 33318144 DOI: 10.1136/gutjnl-2020-322780]

54 **Teo Z**, Sng MK, Chan JSK, Lim MMK, Li Y, Li L, Phua T, Lee JYH, Tan ZW, Zhu P, Tan NS. Elevation of adenylate energy charge by angiopoietin-like 4 enhances epithelial-mesenchymal transition by inducing 14-3-3γ expression. *Oncogene* 2017; **36**: 6408-6419 [PMID: 28745316 DOI: 10.1038/onc.2017.244]

55 **Sho S**, Court CM, Winograd P, Russell MM, Tomlinson JS. A prognostic mutation panel for predicting cancer recurrence in stages II and III colorectal cancer. *J Surg Oncol* 2017; **116**: 996-1004 [PMID: 28767131 DOI: 10.1002/jso.24781]

56 **Pickering KA**, Gilroy K, Cassidy JW, Fey SK, Najumudeen AK, Zeiger LB, Vincent DF, Gay DM, Johansson J, Fordham RP, Miller B, Clark W, Hedley A, Unal EB, Kiel C, McGhee E, Machesky LM, Nixon C, Johnsson AE, Bain M, Strathdee D, van Hoof SR, Medema JP, Anderson KI, Brachmann SM, Stucke VM, Malliri A, Drysdale M, Turner M, Serrano L, Myant K, Campbell AD, Sansom OJ. A RAC-GEF network critical for early intestinal tumourigenesis. *Nat Commun* 2021; **12**: 56 [PMID: 33397922 DOI: 10.1038/s41467-020-20255-4]

57 **Stevenson L**, Allen WL, Turkington R, Jithesh PV, Proutski I, Stewart G, Lenz HJ, Van Schaeybroeck S, Longley DB, Johnston PG. Identification of galanin and its receptor GalR1 as novel determinants of resistance to chemotherapy and potential biomarkers in colorectal cancer. *Clin Cancer Res* 2012; **18**: 5412-5426 [PMID: 22859720 DOI: 10.1158/1078-0432.CCR-12-1780]